Available online at www.sciencedirect.com

SciVerse ScienceDirect

Procedia CIRP 8 (2013) 141 – 146

www.elsevier.com/locate/procedia

14th CIRP Conference on Modeling of Machining Operations (CIRP CMMO)

A finite element model of ultrasonically assisted drilling in carbon/epoxy composites

Vaibhav A. Phadnis[1,*], Anish Roy, Vadim V. Silberschmidt

Wolfson School of Mechanical and Manufacturing Engineering, Loughborough University, LE11 3TU, Leics, UK

* Corresponding author. Tel.:+44 (0)1509 227 634. *E-mail address*: v.a.phadnis@lboro.ac.uk.

Abstract

Ultrasonically assisted drilling (UAD) is a novel machining technique suitable for drilling difficult-to-machine materials such as carbon/epoxy composites, where ultrasonic vibrations are superimposed on the tip of the revolving drill bit. Recently, UAD has been shown to possess several advantages in comparison to conventional drilling, including a reduced thrust force and torque, reduced drilling-induced damage and overall improvement in roundness and surface finish of the drilled hole. Here, a finite element model of UAD in carbon/epoxy composite is presented. This model accounts for volumetric and thermal softening phenomena in the workpiece material under the influence of localized vibro-impacts, which is a characteristic feature of UAD. The model was implemented in Abaqus/Explicit and validated with results from experiments, demonstrating a reasonable correlation between them. A parametric study was also carried out to examine the effect of variation in intensity of ultrasonic energy on the extent of softening in the carbon/epoxy composite for UAD.

Keywords: Carbon/epoxy composite; Finite element analysis; Ultrasonically assissted drilling

1. Introduction

Carbon fibre-reinforced polymer (CFRP) composites are widely used in aerospace and automobile industries and several other structural applications owing to their superior mechanical and physical properties. CFRPs outperform structural metals in durability, high strength-to-weight ratio, stiffness and density [1-4]. In spite of these advantages, machining CFRPs is cumbersome due to highly abrasive carbon fibres, low thermal conductivity of epoxy and a weak interfacial bond between reinforced fibres and matrix.

Parts made of CFRP composite are manufactured to the required final shape, though machining cannot be avoided to assemble individual components. Holes need to be drilled to facilitate riveting and bolting of machined components; to serve this purpose; conventional drilling (CD) methods are often adopted. Apart from poor geometric tolerance and surface finish, CD can initiate various damage modes in CFRPs such as matrix cracking, burr formation, interfacial de-bonding, delamination and fibre pull-out [1, 4, 11]. Consequently, the load-carrying capacity of composite structure is affected. Additionally, rapid tool wear is caused by abrasive carbon fibres resulting in frequent tool replacement. To overcome these issues, a need for alternative drilling technique is recognised.

Ultrasonically Assisted Drilling (UAD) is a hybrid machining technique, which has been used to improve machining of conventional metals and advanced composites in the recent past [2-10]. In UAD, high-frequency (typically in excess of 20 kHz) vibrations generated by a piezoelectric transducer are superimposed on a rotating standard twist drill bit in the axial direction, to enhance the cutting process [5,8]. There are several advantages of UAD over CD such as reduction in drilling forces and torque, better surface finish, low tool wear and elimination in burr formation [11-13]. In drilling CFRPs, drilling forces have a direct effect on damage induced in these composites. Hence it is considered to be the primary parameter affecting quality

doi:10.1016/j.procir.2013.06.079

of a drilled hole [1, 4, 11]. In the experimental study conducted by Hochen and Liu [10] it was concluded that ultrasonic machining had viable advantages over conventional machining processes e.g. force and torque reduction. Wang [11] performed several experiments involving UAD in CFRP. Using a vibration frequency of 300 Hz to excite a high-speed-steel (HSS) and carbide drill bits of 0.5 mm diameter; it was observed that thrust forces were reduced relative to those in CD. Babitsky and Astashev [5, 8] reported that in UAD, torsional vibration does not contribute much to thrust force reduction in comparison to the axial direction. Very few researchers have attempted to model a UAD process using a finite element (FE) technique due to the complexity involved in modelling of such processes and the extent of computational resources required, though analytical model [14] to calculate thrust forces in UAD can be found.

This paper presents development of a FE model of UAD in CFRP composite using general purpose software - Abaqus 6.11. The experimental results from our previous work [2-4] are presented for the validation purpose.

2. FE model of UAD in CFRP

2.1 Background and assumptions

UAD includes superposition of ultrasonic vibration onto the relative cutting motion between a drill bit and the workpiece drilled. This collective effect results in the substantial reduction in the drilling forces and torque [2-6]. Based on the preliminary observations from our UAD experiments [2-4], a CFRP workpiece undergoes plastic deformation under the influence of ultrasonic vibrations, the extent of which depends on the intensity of vibrations, resulting in softening the workpiece in the process zone. Additionally, surface temperature of the CFRP workpiece often exceed glass- transition temperature of thermoset epoxy polymer matrix (170 - 190^0C), resulting in matrix burning. The reduced thrust force and torque observed in UAD is claimed to be due to the combined influence of ultrasonic vibrations giving rise to the vibro-impact and localised heating phenomena. In this context, we define ultrasonic softening as, the phenomenon in which ultrasonic vibrations reduce the apparent static stress necessary for material to undergo permanent inelastic deformation.

In this work, a parametric modelling approach was used to account for acoustic (ultrasonic) and thermal softening phenomena during inelastic deformation of the CFRP workpiece. The behaviour of CFRP laminate in elastic regime was defined using the Hill's [13-14] potential theory for anisotropic materials together with the rate-independent plasticity criterion incorporating effects of ultrasonic softening. An element-removal scheme was used based on the shear damage-initiation criterion to replicate the hole-making process. The temperature rise due to plastic straining was modelled assuming adiabatic conditions. It should be noted that the temperature is a plastic strain work conjugate in the adiabatic system; hence an element was also removed from the mesh when instantaneous temperature reaches the glass transition limit of the epoxy matrix (irrespective of instantaneous plastic strain reaching the fracture strain), thus effectively softening the material at macroscale.

- The primary assumptions of this material model are, Instantaneous intensity of ultrasonic vibrations is proportional to plastic strain induced in the CFRP laminate. It is defined in terms of ultrasonic energy per unit time transferred to the workpiece and is a function of instantaneous contact pressure between the chisel edge of the drill bit and the workpiece, the frequency and amplitude of vibration.
- The strain-rate dependence of CFRP laminate, especially in transverse and through-thickness directions pertaining to matrix dominance, is small enough to be neglected owing to a low loading rate.
- The temperature rise in CFRP laminate during its interaction with the vibrating drill tip is mainly due to plastic strain developed locally.

2.2 Constitutive material model

The workpiece material used in this study was commercially available quasi-isotropic laminate M21/T700 of thickness 10 mm with individual ply thickness of 0.25 mm. The details on the stack sequence and mechanical properties of CFRP laminate employed in these simulations can be found in Phadnis *et al.* [4].

The thermo-mechanical plasticity model proposed in this work is based on the quadratic yield criterion for anisotropic materials by Hill [13-14] and non-linear isotropic hardening rule for rate-independent plasticity. The constitutive equations of this model for uniaxial loading are as follows:

The total strain tensor during deformation is the sum of elastic strain tensor and plastic strain tensor, given by,

$$\boldsymbol{\varepsilon} = \boldsymbol{\varepsilon}^{el} + \boldsymbol{\varepsilon}^{pl}. \qquad (1.1)$$

The elastic part of stresses is computed using a constitutive stress-strain relationship;

$$\boldsymbol{\sigma} = \mathbf{C} \,.\, \boldsymbol{\varepsilon} = (\boldsymbol{\varepsilon}^{el} - \boldsymbol{\varepsilon}^{pl}), \qquad (1.2)$$

where, $\boldsymbol{\sigma}$ and $\boldsymbol{\varepsilon}$ are the second-order elastic stress and strain tensors while $\mathbf{C}$ is the fourth-order stiffness tensor. The yield function [13] for orthotropic CFRP

material in rectangular Cartesian stress components is given by

$$f(\boldsymbol{\sigma}) = \sqrt{\begin{matrix} F(\bar{\sigma}_{22}-\bar{\sigma}_{33})^2 + G(\bar{\sigma}_{33}-\bar{\sigma}_{11})^2 + \\ H(\bar{\sigma}_{11}-\bar{\sigma}_{22})^2 + 2L\bar{\sigma}_{23}^2 + 2M\bar{\sigma}_{31}^2 \\ +2N\bar{\sigma}_{12} \end{matrix}} = \left|\boldsymbol{\sigma}^{y}\right| + R, \tag{1.3}$$

where F, G, H, L, M and N are constants, obtained from the following equations.

$$F = \frac{(\sigma^0)^2}{2}\left(\frac{1}{\bar{\sigma}_{33}^2}+\frac{1}{\bar{\sigma}_{11}^2}+\frac{1}{\bar{\sigma}_{22}^2}\right) = \frac{1}{2}\left(\frac{1}{R_{33}^2}+\frac{1}{R_{11}^2}+\frac{1}{R_{22}^2}\right),$$

$$G = \frac{(\sigma^0)^2}{2}\left(\frac{1}{\bar{\sigma}_{22}^2}+\frac{1}{\bar{\sigma}_{33}^2}+\frac{1}{\bar{\sigma}_{11}^2}\right) = \frac{1}{2}\left(\frac{1}{R_{22}^2}+\frac{1}{R_{33}^2}+\frac{1}{R_{11}^2}\right),$$

$$H = \frac{(\sigma^0)^2}{2}\left(\frac{1}{\bar{\sigma}_{11}^2}+\frac{1}{\bar{\sigma}_{22}^2}+\frac{1}{\bar{\sigma}_{33}^2}\right) = \frac{1}{2}\left(\frac{1}{R_{11}^2}+\frac{1}{R_{22}^2}+\frac{1}{R_{33}^2}\right),$$

$$L = \frac{3}{2}\left(\frac{\tau^0}{\bar{\sigma}_{23}}\right)^2 = \frac{3}{2R_{23}^2},$$

$$M = \frac{3}{2}\left(\frac{\tau^0}{\bar{\sigma}_{13}}\right)^2 = \frac{3}{2R_{13}^2},$$

$$N = \frac{3}{2}\left(\frac{\tau^0}{\bar{\sigma}_{12}}\right)^2 = \frac{3}{2R_{12}^2}. \tag{1.4}$$

Here $\bar{\sigma}$ is the measured yield stress when applied as the only non-zero stress component, σ^0 is the initial yield stress and τ^0 is the shear stress at yield such that, $\tau^0 = \sigma^0/\sqrt{3}$. R_{ij} are anisotropic yield ratios and can be calculated from the CFRP yield strengths. $\boldsymbol{\sigma}^{y}$ is the size of an initial yield surface, while R is the isotropic hardening term:

$$R = \sigma^0(\boldsymbol{\varepsilon}^{pl}, \dot{\theta}). \tag{1.5}$$

Plastic strain during deformation is defined as

$$\boldsymbol{\varepsilon}^{pl} = D\left(\frac{\bar{\sigma}}{\sigma^0}-1\right), \text{ for } \bar{\sigma} \geq \sigma^0, \tag{1.6}$$

where $\bar{\sigma}$, σ^0, $\boldsymbol{\varepsilon}^{pl}$, and D are yield stress at non-zero plastic stress, static yield stress, plastic strain and softening parameter respectively. D is defined as $D = D(\psi, \dot{\theta})$ where ψ is ultrasonic energy per unit time and $\dot{\theta}$ is the temperature gradient due to work done towards plastic straining in an adiabatic system. It should be noted that ultrasonic energy per unit time, ψ transmitted to the CFRP surface in the process zone is defined as,

$$\psi = p_c . f_u . a_u . A_c \tag{1.7}$$

where p is the instantaneous contact pressure exerted by the chisel edge of the drill on the CFRP surface; f_u and a_u are the frequency and amplitude of ultrasonic vibration respectively. The standard jobber carbide twist drill (Fig. 4) was used in simulations; the details about drill geometry can be found in [2-4]. The contact pressure was a direct function of the chisel edge geometry. The magnitude of ψ was calculated using (1.7) for the feed rate of 8 mm/min and spindle speed of 40 rpm. The area of contact and corresponding contact pressure was obtained through a number of drilling simulations.

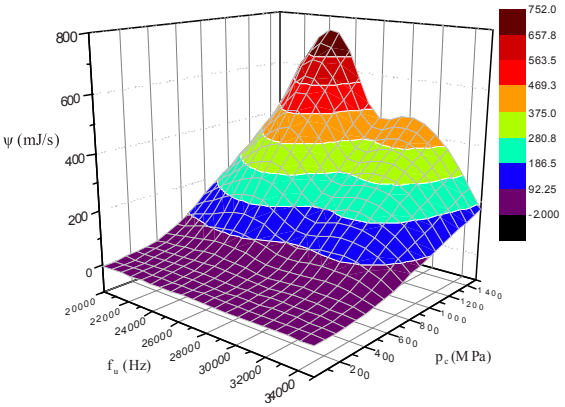

Fig.1. Effect of f_u on ψ (Drill feed 8 mm/min, spindle speed 40 rpm, amplitude of vibration 12 µm peak-to-peak)

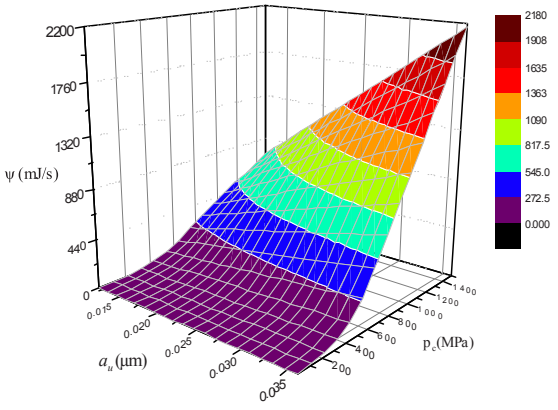

Fig.2. Effect of a_u on ψ (Drill feed 8 mm/min, spindle speed 40 rpm, frequency of vibration 25 kHz)

The effect of a range of frequency and amplitude of ultrasonic vibration on the magnitude of ultrasonic energy per unit time is shown in Fig. 1 and Fig. 2 respectively.

2.3 Adiabatic heat transfer

Heat generation caused by mechanical work associated with plastic straining was modelled in an adiabatic system. The ultrasonic frequency used in these simulations was 27.8 kHz resulting in rapid accumulation of ultrasonic energy in a highly localised regime in a very short period of time. Hence it was assumed that inelastic deformation due to plastic straining occurs so rapidly that heat had hardly any time to diffuse through, and, thus, adiabatic analysis was sufficient to model the temperature rise in this local regime. The model assumed that plastic straining gives rise to a heat flux per unit volume, r^{pl} such that;

$$r^{pl} = \eta\sigma : \dot{\varepsilon}^{pl}, \tag{1.8}$$

where η is the constant inelastic heat coefficient, σ is the instantaneous stress state and $\dot{\varepsilon}^{pl}$ is the plastic strain rate.

2.4 Element-removal scheme

Previous UAD experiments preformed on CFRP composite at Loughborough University, UK yielded quasi-continuous chips instead of brittle powder as would be normally expected, emphasising the effect of underlying softening phenomenon. The results showing chip formation in this process can be found in Makhdum *et al.* [2].

Here, simulations of a hole-generation process in CFRP with UAD were accomplished with the help of the element removal scheme in Abaqus/Explicit [16] and chip formation was not modelled. This scheme was based on the fracture mechanism initiated by shear damage and damage evolution linked to the energy dissipation during degradation of material's stiffness. The in-built Abaqus shear-damage criterion [16] utilised here is a phenomenological model for predicting the onset of damage due to shear-band localisation. It assumes that the equivalent plastic strain at the onset of damage $\tilde{\varepsilon}_s^{pl}$ is a function of the shear stress ratio and instantaneous plastic strain such that,

$$\tilde{\varepsilon}_s^{pl} = \tilde{\varepsilon}_s^{pl}(\chi_S, \tilde{\varepsilon}^{pl}), \tag{1.9}$$

where χ_S is a shear stress ratio:

$$\chi_S = \frac{\tau_S}{\tau_{\max}}. \tag{1.10}$$

Here, τ_S is the total accumulated shear stress at the integration point of an element and $\tau_{\max}$ is the corresponding maximum shear stress. The criterion for damage initiation is met when the following condition is satisfied:

$$\omega_s = \int \left(\frac{1}{\tilde{\varepsilon}_s^{pl}(\chi_S, \tilde{\varepsilon}^{pl})} \right) d\left(\tilde{\varepsilon}^{pl}\right) = 1 \quad , \tag{1.11}$$

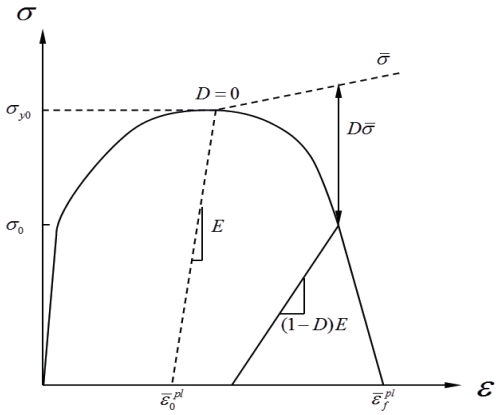

Fig.3. Stress-strain curve with progressive damage behaviour

where ω_s is a state variable that increases monotonically with plastic deformation proportional to the incremental variation in the equivalent plastic strain. The characteristic stress-strain behaviour of a material under uni-axial loading that undergoes progressive damage is shown in Fig.3. In case of the elastic-plastic material this damage can be decomposed into two parts; softening of the yield stress and degradation of the elastic modulus. The solid curve in Fig. 3 represents the damaged stress-strain response, whereas the dashed line represents the undamaged behaviour. σ_{yo} and $\bar{\varepsilon}_0^{pl}$ are yield stress and equivalent plastic strain at the onset of damage, while $\bar{\varepsilon}_f^{pl}$ is the equivalent plastic strain at failure, also known as *fracture strain*.

When material undergoes damage, the stress-strain relationship fails to accurately present its behaviour because of a strong mesh dependency linked to the strain localisation. Hence a different approach is required to trace the strain softening branch of the stress-strain curve. Thus, Hillerborg's fracture energy approach [15] was employed in this model, which eventually helped to reduce mesh dependency by formulating a stress-displacement response after damage initiation. The fracture energy was idealised as work required to open a unit area of a crack and expressed as

$$G_f = \int_{u_{pl}}^{u_{pl}^f} \sigma_y \, . \, d\left(\bar{u}^{pl}\right), \tag{1.12}$$

where $\bar{u}^{pl}$ is the equivalent plastic displacement and can be considered as fracture energy conjugate of yield stress after the damage initiation : $\bar{u}^{pl} = 0$ at damage initiation and $\bar{u}^{pl} = L\bar{\varepsilon}^{pl}$ after it. Here L is the

characteristic length of an element in a meshed body that depends on its geometry and formulation. D is the overall damage parameter: at damage initiation $D = 0$, while at complete damage $D = 1$. The residual elastic modulus E_r, after damage initiation can be calculated as:

$$E_r = (1 - D).E. \quad (1.13)$$

Evolution of the damage variable $\dot{d}$ associated with a relative plastic displacement was specified in a linear form as,

$$\dot{d} = \frac{\bar{u}^{pl}}{\bar{u}_f^{pl}}, \quad (1.14)$$

where $\bar{u}_f^{pl}$ is the equivalent plastic displacement at failure and can be calculated as

$$\bar{u}_f^{pl} = \frac{2G_f}{\sigma_{y0}}. \quad (1.15)$$

2.5 FE model setup

2.5.1 Geometric modelling and boundary conditions

A 3D geometry of 6 mm twist drill with a point angle of 118° and helix angle of 31° was modelled in Abaqus [16]. The drill was modelled as a rigid body. The mesh was optimized to reduce the computational cost without compromising accuracy. A mesh size of CFRP work piece was refined in the immediate vicinity of the drilled area to capture high stress gradients during the drilling process. Elements in the refined cylindrical zone were removed when the failure criterion was met during simulations using element deletion discussed in section 2.4. The CFRP laminate was fixed at all four vertical faces, while the drill was constrained to rotate only about its own axis with a specified speed and fed vertically downwards into the work piece. The FE analysis was performed with experimentally optimised drilling parameters: spindle speed of 40 rpm, feed rate of 8 mm/min, vibration frequency of 27.8 kHz, peak-to-peak vibration amplitude of 12 µm. A time-dependent sinusoidal movement representing a cycle of ultrasonic vibration was imposed on the drill in the axial direction to incorporate the vibrating boundary condition. Each wave consisted of 27,800 periodic sampling points for one second of simulated period of drilling.

The drill is thus vibrated along the vertical direction as well as rotated about its own axis independently. Contact between the twist drill and the CFRP laminate was defined with general contact algorithm. A coefficient of dry friction at the interface between drill's cutting edge and laminate was assumed to be 0.03 based on the work by Lucas et al. [12].

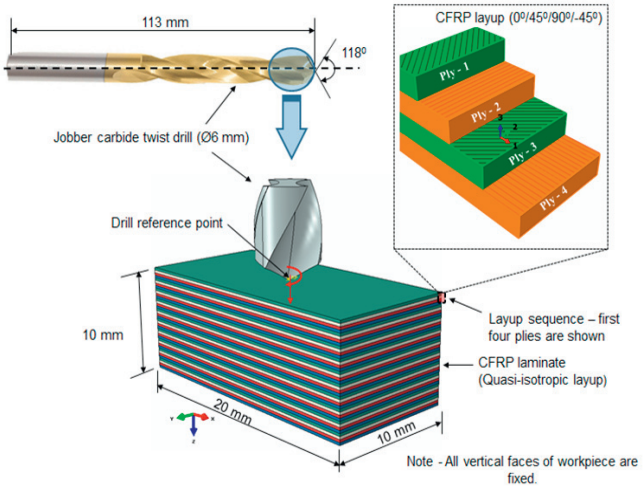

Fig.4. Finite element model of UAD in M21/T700 composite laminate

2.5.2 Choice of finite elements

The Hill's potentential mainly depends on the deviatoric stress components and the plastic response becomes almost incompressible [16, 17]. The finite elements were selected to accommodate this incompressibility. Adiabatic conditions were assumed.

In an adiabatic heat transfer analysis, the heat equation solved at each integration point is given by,

$$\rho c(\theta)\dot{\theta} = r^{pl}, \quad (1.16)$$

where r^{pl} the heat flux per unit volume due to plastic strain is, ρ is the material density $c(\theta)$ is specific heat and $\dot{\theta}$ is the instantaneous temperature gradient. The adiabatic heat was calculated using material properties and no external heat flux was added into the system, thus temperature degrees of freedom were not required. In this simulation, eight-node, first-order, one-integration point hexahedral elements of type C3D8R were used. The CFRP laminate was meshed with 820000 elements with the smallest element size of 5 µm. The drill was modelled with four-node, 3D discrete rigid elements of type C3D4 and meshed with 35000 elements, with the smallest element size of 125 µm.

3. FE Results

The results obtained from FE simulations comprise the average of peak thrust force and torque for UAD in CFRP laminate. The thrust force and torque obtained under similar machining parameters and material properties with conventional drilling technique [5-7] are

also presented for the comparison purpose and are shown in Fig. 5 and Fig. 6.

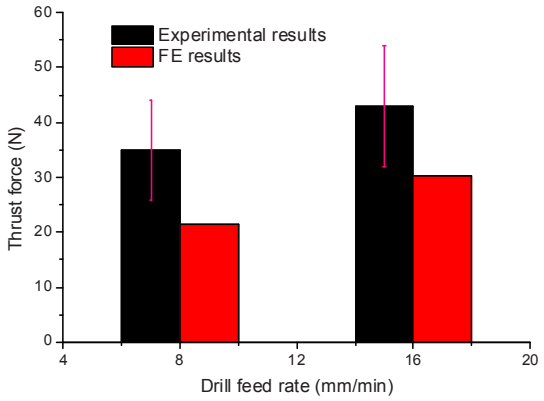

Fig.5. Comparison of peak thrust force using experiments and FEA ($a = 12\ \mu$m, $f = 27.8$ kHz)

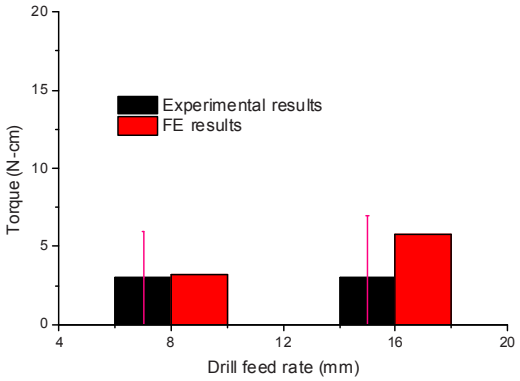

Fig.6. Comparison of peak torque using experiments and FEA ($a = 12\ \mu$m, $f = 27.8$ kHz)

4. Conclusions

A finite element model of UAD in CFRP is developed. A constitutive material model suitable to model both volumetric and thermal softening in CFRP laminate under ultrasonic vibrations is proposed. The validated FE model showed good co-relation with the experimental results, demonstrating potential capabilities of this model to predict features of UAD.

References

[1] R Zitoune, V Krishnaraj, F Collombet, 2012. Influence of machining parameters and new nano-coated tool on drilling performance of CFRP/aluminium sandwich. Composites Part B: Engineering 43:1480-8.

[2] F Makhdum, LT Jennings, A Roy, VV Silberschmidt. 2012. Cutting forces in ultrasonically assisted drilling of carbon fibre-reinforced plastics. Journal of Physics: Conference Series.;382(1):012019.

[3] F Makhdum, Dk Nurdiya, A Roy , VV Silberschmidt. 2012. Ultrasonically assisted drilling of carbon fibre reinforced plastics. *Solid State Phenomena*. 188:170-5.

[4] VA Phadnis, F Makhdum, A Roy, VV Silberschmidt. 2012, Experimental and numerical Investigations in conventional and ultrasonically assisted drilling of CFRP Laminate. *Procedia CIRP*. 1:455-9.

[5] VK Astashev, VI Babitsky. 2007. Ultrasonic processes and machines: dynamics, control and applications. Berlin Heidelberg New York: *Springer*.

[6] P Thomas, VI Babitsky. 2007. Experiments and simulations on ultrasonically assisted drilling. *Journal of Sound and Vibration* 308:815.

[7] K Alam, AV Mitrofanov, VV Silberschmidt. 2011. Experimental investigations of forces and torque in conventional and ultrasonically-assisted drilling of cortical bone. *Medical Engineering & Physics* 33:234

[8] VI Babitsky, VK Astashev, A Meadows. 2007. Vibration excitation and energy transfer during ultrasonically assisted drilling. Journal of Sound and Vibration 308:805-14

[9] M Wiercigroch, J Wojewoda, A Krivtsov. 2005. Dynamics of ultrasonic percussive drilling of hard rocks. *Journal of Sound and Vibration* 280:739-57

[10] H Hocheng, NH Taib, CS Liu. 2000. Assessment of ultrasonic drilling of C/SiC composite material. *Composites: Part A*. 31:133-42.

[11] X Wang, L Wang. 2004. Investigation on thrust in vibration drilling of fiber-reinforced plastics. *Journal of Materials Processing Technology*. 148(2):239-44.

[12] M Lucas, A, MacBeath, McCulloch, E Cardoni. 2006. A finite element model for ultrasonic cutting. *Ultrasonics*.44:.503-509.

[13] R Hill. 1990. Constitutive modelling of orthotropic plasticity in sheet metals. *Journal of the Mechanics and Physics of Solids*.;38(3):405-17.

[14] R Hill. 1998. The Mathematical Theory of Plasticity: Clarendon Press.

[15] A Hillerborg.1985. Theoretical basis of a method to determine the fracture energy concrete. *Materials and Structures*. 18(4):291-6.

[16] Abaqus 6.11 User manual 2011. Dassault System. Rhode Islands, US.